

Title	Radial and vertical distributions of radiocesium in tree stems of <i>Pinus densiflora</i> and <i>Quercus serrata</i> 1.5 y after the Fukushima nuclear disaster.
Author(s)	Ohashi, Shinta; Okada, Naoki; Tanaka, Atsushi; Nakai, Wataru; Takano, Shigeyoshi
Citation	Journal of environmental radioactivity (2014), 134: 54-60
Issue Date	2014-08
URL	http://hdl.handle.net/2433/187148
Right	© 2014 Elsevier Ltd.
Type	Journal Article
Textversion	author

1 Radial and vertical distributions of radiocesium in tree stems of *Pinus densiflora* and *Quercus*
2 *serrata* 1.5 y after the Fukushima nuclear disaster

3

4 Shinta Ohashi^{a*}, Naoki Okada^a, Atsushi Tanaka^a, Wataru Nakai^b, Shigeyoshi Takano^b

5 ^aDepartment of Natural Resources, Graduate School of Global Environmental Studies, Kyoto
6 University, Kyoto 606-8501, Japan

7 ^bDepartment of Forest and Biomaterials Science, Faculty of Agriculture, Kyoto University, Kyoto
8 606-8502, Japan

9

10 *Corresponding author

11 Department of Natural Resources, Graduate School of Global Environmental Studies, Kyoto
12 University, Kyoto 606-8501, Japan

13 Tel: +81-75-753-6097

14 E-mail: shinta.res@gmail.com

1 Highlights

- 2 • Radiocesium concentrations in tree stems of pine and oak were determined.
- 3 • Vertical distributions of radiocesium were different between the species.
- 4 • Radial distributions of radiocesium in wood were similar in both species.
- 5 • Radiocesium distributions among stem parts differed between the species.
- 6 • Transportation and allocation of radiocesium would differ between the species.

1 Abstract

2 The radial and vertical distributions of radiocesium in tree stems were investigated to
3 understand radiocesium transfer to trees at an early stage of massive contamination from the
4 Fukushima nuclear disaster. A conifer species (Japanese red pine) and a broad-leaved species
5 (Japanese *konara* oak) were selected to determine whether the radiocesium contamination
6 pattern differs between species. Stem disks were collected at several heights and separated
7 into outer bark, inner bark, and wood. The radiocesium concentration was the highest in the
8 outer bark, followed by that in the inner bark and wood. The vertical distribution of the
9 radiocesium concentration at each stem part differed between the species. The difference
10 between species in radiocesium concentration of the outer bark could be explained by
11 presence or absence of leaves at the time of the disaster. However, the reasons for the
12 differences between species in the radiocesium concentration of the inner bark and wood are
13 unclear. The radial distribution in the wood of the studied species showed a common pattern
14 across stem disk heights and species. However, the radiocesium concentration ratio between
15 sapwood and inner bark was significantly different between species. Although the radial
16 contamination pattern in the wood was similar in the studied species during the early stage of
17 contamination, the radiocesium transport pathway and allocation would be different between
18 the species, and the contamination pattern will likely be different between the species at later
19 stages. Continued investigations are important for understanding the radiocesium cycle and
20 the accumulation of radiocesium in the tree stems of each species.

21

22 Keywords

23 Fukushima, radiocesium, bark, wood, radial distribution, vertical distribution

24

25

26 1. Introduction

27 A considerable amount of radiocesium (^{134}Cs and ^{137}Cs) was emitted into the atmosphere by
28 the Fukushima Dai-ichi nuclear disaster in March 2011. The fallout was largely deposited in
29 forests because they cover much of the land (71% of Fukushima Prefecture). Radiocesium
30 would be well mixed with stable Cs within the biological cycle in forest ecosystems (Yoshida
31 et al., 2004), and ^{137}Cs , which has a long physical half-life (30.2 y), will remain in forest
32 ecosystems for many decades. Therefore, understanding radiocesium dynamics is critical to
33 forest management in contaminated areas. In particular, ^{137}Cs accumulation in trees is one of
34 the most important concerns for timber use and forest decontamination.

35 Radiocesium may enter a tree via root uptake, translocation from the foliar surface, or even
36 from the bark surface (Ertel and Ziegler, 1991; Tagami et al., 2012). In a tree stem,
37 radiocesium is mobile and passes through tree rings (Kohno et al., 1988; Kudo et al., 1993;
38 Momoshima and Bondietti, 1994), resulting in whole-stem contamination. Some radiocesium
39 may form ionic bonds with carboxylic groups in cell walls, the cytoplasm of living cells, and
40 the cell debris of the heartwood, the inner part of wood (Brown, 1964). Because heartwood is
41 composed of dead cells and hence does not function in water transport, radiocesium that
42 transferred to heartwood is likely to remain there for a long time. Parallel distribution of ^{137}Cs
43 to that of ^{40}K in a Japanese cedar (*Cryptomeria japonica*) stem (Kudo et al., 1993) and to
44 those of alkaline metals in Scots pine (*Pinus sylvestris*) stems (Yoshida et al., 2011) suggests
45 that radiocesium transferred to heartwood stayed there and reached to an equilibrium
46 distribution to the elements with similar chemical properties.

47 Previous studies have indicated that the radiocesium distribution among sapwood (the
48 outer part of wood, which transports water and has living cells) and heartwood differs
49 between species. For example, Japanese cedar and cypress (*Chamaecyparis obtusa*)
50 reportedly have higher ^{137}Cs concentration in the heartwood than in the sapwood (Kohno et

51 al., 1988), whereas Scots pine is reported to have a higher ^{137}Cs concentration in the sapwood
52 than in the heartwood (Thiry et al., 2002; Yoshida et al., 2011). Soukhova et al. (2003)
53 reported different ^{137}Cs distributions in Scots pine and silver birch (*Betula pendula*) and
54 attributed the difference to the different radial ray compositions of those species.

55 Although ^{137}Cs accumulation in tree stems is understood to a certain extent, further
56 research is needed to improve our understanding and ability to predict ^{137}Cs accumulation in
57 wood. Research into the early stages of contamination is particularly lacking. Moreover, for
58 proper forest management in Fukushima, native species growing in the local environment
59 must be studied. Kuroda et al. (2013) reported that ^{134}Cs and ^{137}Cs were detected in the
60 heartwood of three species (*Pinus densiflora*, *Quercus serrata*, and *Cryptomeria japonica*)
61 collected from Fukushima forests half a year after the Fukushima Dai-ichi nuclear accident.
62 This fact indicates that there is rapid inflow of radiocesium to tree stems and rapid
63 translocation to heartwood, highlighting the importance of research into the early stages of
64 contamination.

65 In the present study, we investigated the radial and vertical distributions of radiocesium in
66 tree stems of two dominant species, Japanese red pine (*P. densiflora* Sieb. & Zucc.) and
67 Japanese *konara* oak (*Q. serrata* Thunb.), 1.5 y after the Fukushima Dai-ichi nuclear disaster,
68 focusing on whether the radiocesium transfer pattern differs between species.

69

70 2. Material and methods

71 2.1. Study sites and sampling

72 A Japanese red pine forest (pine forest) and a deciduous broad-leaved forest (oak forest) in
73 Kawauchi Village, about 20 km southwest of the Fukushima Dai-ichi Nuclear Power Plant,
74 were selected for the study (Fig. 1). Pine and oak forests were representative forest types in
75 the village. Samples were collected from trees that were adjacent to a 40 m × 40-m census

76 plot in the pine forest (520 m above sea level) and a 50 m × 30-m census plot in the oak
77 forest (530 m above sea level). In the pine plot, tree density (diameter at breast height > 5 cm)
78 was 1,513 ha⁻¹ and Japanese red pine (*P. densiflora*) accounted for 73% of the trees. The
79 forest canopy was completely dominated by the red pines, but was not fully closed; the
80 remaining 27% of the trees in the plot vegetated in the understory (e.g., *Toxicodendron*
81 *trichocarpum* 5%, *Q. serrata* 4%, and *Swida controversa* 4%). In the oak plot, the tree
82 density was 1,413 ha⁻¹ and Japanese *konara* oak (*Q. serrata*) accounted for 38% of the trees,
83 followed by Japanese clethra (*Clethra barbinervis*; 12%), Japanese wild cherry (*Cerasus*
84 *jamasakura*; 6%), sawtooth oak (*Q. acutissima*; 5%), and Japanese *mizunara* oak (*Q.*
85 *crispula*; 5%). The forest canopy was dominated by *Q. serrata*, *Q. acutissima*, and *Q.*
86 *crispula*, but was not closed, forming a multistory vertical structure. The air dose rate was 0.2
87 μSv h⁻¹ at the pine forest and 1.8 μSv h⁻¹ at the oak forest, as measured in late July 2012 at 1
88 m above the ground using an ionization chamber-type survey meter (ICS-331B; Hitachi
89 Aloka Medical Ltd., Tokyo, Japan). The ¹³⁷Cs contamination in soil (the sum of the
90 contamination found in the litter layer, fermentation layer, humus layer, and mineral soil) was
91 1.1 × 10⁵ Bq m⁻² (a standard deviation (σ) = 3.0 × 10⁴ Bq m⁻²) at the pine plot and 1.5 × 10⁵
92 Bq m⁻² (σ = 4.9 × 10⁴ Bq m⁻²) at the oak plot in September 2012. These values were the
93 means of three sampling points collected diagonally at each plot and were used to calculate
94 the aggregated transfer factor (T_{ag} ; m² kg⁻¹) from soil to tree. The sampling points were at
95 least 2 m away from tree stems in order to avoid thick roots. The litter layer, fermentation
96 layer and humus layer were collected from a 50 cm × 50-cm area at each point. The mineral
97 soil (brown forest soil) to a depth of 20 cm was collected using cylindrical soil samplers.

98 Three pines (*P. densiflora*) and three oaks (*Q. serrata*) that were adjacent to the respective
99 census plots were logged in early September 2012. The diameter at breast height (DBH), tree
100 height, and age of each tree are shown in Table 1. The trees were selected from individuals of

101 different diameter classes growing in the dominant tree layer in order to represent the
102 diameter distribution of each species. The diameters of both species in their respective census
103 plots showed normal distributions: mean DBH of *P. densiflora* in the pine plot was 24.5 cm
104 ($\sigma = 5.8$ cm, $n = 175$) and that of *Q. serrata* in the oak plot was 19.8 cm ($\sigma = 5.8$ cm, $n = 82$).
105 All pines and oaks selected were considered to be mature as the youngest was 36 y of age.
106 Disk samples that were approximately 5 cm thick were removed from each logged stem at 0.3,
107 1.3, 5, and 10 m above ground. Additional disk samples were removed from pines at 15 m
108 above ground, from a short oak tree at 7.5 m, and from tall oaks at 12.5 m.

109

110 2.2. Sample preparation and analysis

111 The disks were separated into three parts: outer bark (cork), inner bark (phloem), and wood
112 (xylem). The outer bark was removed from the disks using a chisel, after which the inner bark,
113 including the cambium, was removed. The disks collected at the following stem heights were
114 used for xylem analysis: pine1 (1.3 and 15 m), pine2 (1.3, 5, 10, and 15 m), pine3 (1.3 and 15
115 m), oak1 (1.3 and 7.5 m), oak2 (1.3, 5, and 10 m), and oak3 (1.3 and 10 m). Each disk was
116 further separated along tree-ring boundaries into sub-samples of several rings each. Each
117 sub-sample weighed ca. 50 g (dry mass at 80°C). This sample separation resulted in sufficient
118 material for γ -ray spectrometry and provided enough resolution for investigation of the radial
119 migration of radiocesium in the tree stems. Distances from the pith to each separated ring
120 boundary were measured along four radii and their average was used as the distance between
121 pith and ring boundary. The distance of the sapwood–heartwood boundary from the pith was
122 measured in the same way.

123 All samples, except mineral soil samples, were ground using a Wiley mill before packing
124 into plastic containers. Mineral soil samples were packed after drying for at least 7 d, and

125 sieving with 2-mm mesh. About 1 g of each sample was dried at 80°C for 48 h to calculate
126 the dry mass.

127 The radioactivity of ^{134}Cs (605 keV) and ^{137}Cs (662 keV) in tree and soil samples were
128 measured using a high-purity Ge semiconductor detector (Tennelec, Tennessee, USA) at the
129 Radioisotope Research Center of Kyoto University. The γ -ray detection efficiency was
130 calibrated with the standard, which was prepared by using a reference standard QCY.44
131 supplied by Radiochemical Center Ltd., Amersham (Veronica et al., 1992), and provided by
132 the Radioisotope Research Center, Kyoto University. The measuring time was 7,200–50,000
133 s, depending on the radioactivity of each sample. The detection limit of each radionuclide
134 was calculated using Cooper's equation (Cooper, 1970; eq. 8, $A_m = 3$). The radioactivity was
135 decay-corrected to September 1, 2012. All radiocesium concentrations in the present study
136 are shown in dry mass (at 80°C) base.

137

138 3. Results and Discussion

139 3.1. Radiocesium distribution among stem parts

140 In both species, radiocesium concentration (Bq kg^{-1}) was the highest in the outer bark,
141 followed by that in the inner bark and whole wood (Table 2). The ratio of ^{134}Cs to ^{137}Cs was
142 about 0.6 in most samples. The burden of radiocesium (Bq) in each disk was also the largest
143 in the outer bark, followed by that in the whole wood and inner bark. The burdens followed
144 the same order at all analyzed heights. The concentration was reportedly the highest in the
145 inner bark or cambium about 10 y after the Chernobyl accident (Thiry et al., 2002; Yoshida et
146 al., 2011). Thiry et al. (2002) showed that 7% of the total ^{137}Cs in the stem was distributed in
147 the outer bark, 18% in the inner bark, and 75% in the whole wood of 58-year-old Scots pine
148 trees 12 y after the Chernobyl accident. In the present study, 74% was distributed in the outer
149 bark, 6% in the inner bark, and 20% in the whole wood of Japanese red pine trees (collected

150 at 1.3 m above the ground). Thus, 1.5 y after the disaster, the remaining surface
151 contamination was still serious and further transfer to the interior of the stem might occur.

152

153 3.2. Vertical distribution of radiocesium in each stem part

154 The vertical distribution of the radiocesium concentration in the outer bark was different
155 between the species (Fig. 2). In oaks, the radiocesium concentration in the outer bark was
156 higher in the upper stem than in the lower stem and had a significant correlation with
157 sampling height ($n = 14$, $p < 0.001$). In pines, however, the radiocesium concentration in the
158 outer bark did not vary significantly with sampling height. The remarkably high deposition
159 on the upper part of the outer bark of oaks might have occurred because the leafless canopy at
160 the time of the initial massive deposition promoted direct capture of radiocesium by the bark
161 surface.

162 The vertical distribution of radiocesium concentration in the inner bark was almost uniform
163 in both species. However, the distribution pattern differed among individual oaks, whereas
164 the distribution pattern was similar among individual pines: although oak1 and oak2 did not
165 show a significant correlation between radiocesium concentration and sampling height, oak3
166 did ($n = 5$, $p < 0.01$). This difference between species in individual variation may be due to
167 branching. The pines had living branches only at the top part of the main stem, whereas the
168 oaks had living branches at multiple heights. Accordingly, in the oaks, radiocesium in the
169 foliage would be supplied to the main stem at multiple heights via the inner bark (phloem),
170 and that might result in individual differences in radiocesium vertical distribution patterns.

171 In the wood of both species, there was a significant correlation between radiocesium
172 concentration and sampling height (Fig. 3). The radiocesium concentration in the whole wood
173 of the pines was slightly higher in the upper stem than in the lower stem (regression
174 coefficient = 1.1). On the other hand, that in the oaks was significantly higher in the upper

175 stem than in the lower stem (regression coefficient = 7.4). The slight increase of radiocesium
176 concentration toward the upper stem of the pines can be explained well by the vertical
177 variation in heartwood ratio. The upper stem contained less heartwood than the lower stem,
178 and the sapwood contained more radiocesium than the heartwood. In addition, the
179 radiocesium concentration in the sapwood of the pines was almost constant across sampling
180 heights. Therefore, the radiocesium contamination to the stem wood of the pines likely
181 progresses uniformly regardless of stem height. This agrees with the report by Thiry et al.
182 (2002), ¹³⁷Cs concentrations in the stem wood of Scots pines 12 y after the Chernobyl
183 accident were largely unaffected by stem height. On the other hand, the vertical distribution
184 of radiocesium in the oaks cannot be explained by the vertical variation in heartwood ratio
185 alone because in this species, the sapwood in the upper stem had a significantly higher
186 radiocesium concentration than that in the lower stem. One possible reason for the
187 relationship between radiocesium concentration and height in oaks is direct radiocesium
188 transfer from the outer bark. Several studies have suggested the possibility of radiocesium
189 absorption by bark (Ertel and Ziegler, 1991; Tagami et al., 2012). The remarkably high
190 radiocesium concentrations in the outer bark and whole wood in the upper part of oaks and
191 their significant correlation ($n = 7$, $p < 0.01$) imply the possibility of bark absorption;
192 however, this must be demonstrated in a future study. Although the reason remains unclear,
193 the vertical contamination pattern differs between the species examined.

194

195 3.3. Radial distribution of radiocesium in wood

196 The radial distribution of the radiocesium concentration had a similar pattern among the
197 analyzed heights and species (Figs. 4 and 5). The concentration was (1) the highest at the
198 outermost part; (2) almost uniform throughout the sapwood, except for the outermost part;
199 and (3) reduced toward the center in the heartwood.

200 One reason for the relatively high concentration in the outermost part of the stems is that
201 the contamination occurred recently. In addition, radiocesium may be preferentially
202 translocated to the young growing part of stem wood, as suggested by the analysis of Scots
203 pine 12 y after the Chernobyl accident (Yoshida et al., 2011).

204 The uniform radiocesium concentration observed throughout the sapwood would be due to
205 both diffusion and active transport. Thiry et al. (2002) indicated that the distribution pattern
206 of ^{137}Cs in sapwood is in good agreement with the distribution of free water in wood, which
207 increases from the inner sapwood to the outer sapwood. In addition, active radial transport
208 through rays must be taken into account. The radial solute exchange between xylem and
209 phloem occurs via the rays (van Bel, 1990). In Japanese cedar, alkali metals are transported
210 actively from the sapwood to the outer heartwood via rays (Okada et al., 2012). Moreover,
211 Soukhova et al. (2003) explained that the radial ^{137}Cs distribution in pine differs from that in
212 birch because of the different ray composition between these species. The proportion of
213 tracheid and parenchyma cells in the rays affects radial transport characteristics. In the
214 present study, the radiocesium concentration ratio of sapwood to inner bark was significantly
215 higher in oaks than in pines (Welch's t-test; $p < 0.001$), at 0.23 ($\sigma = 0.041$, $n = 7$) in oaks and
216 0.088 ($\sigma = 0.026$, $n = 7$) in pines. This difference seems to suggest that oaks transport more
217 radiocesium from phloem to sapwood via rays than do pines. The active radial transport
218 through rays is an important point that must be considered in a future study.

219 In the heartwood, the movement of radiocesium toward the center must be caused by
220 diffusion alone because there are no living cells in heartwood. The decrease in the
221 radiocesium concentration in proportion to the distance from the sapwood–heartwood
222 boundary in both species confirms movement by diffusion. However, species-specific radial
223 distribution patterns of ^{137}Cs concentration might appear after several years. Uniform
224 distribution patterns have also been observed in Scots pines (Thiry et al., 2002; Soukhova et

225 al., 2003; Yoshida et al., 2011), whereas increasing radiocesium concentration toward the
226 center of the heartwood has been reported for Japanese cedar, cypress (Kohno et al., 1988),
227 and birch (Soukhova et al., 2003). These different patterns of ^{137}Cs accumulation would result
228 from different radial distributions of water, different heartwood compositions, and different
229 processes of heartwood formation between species or individuals. These factors must be
230 observed carefully and reviewed periodically after radioactive fallout in order to understand
231 the mechanism of radiocesium accumulation in heartwood.

232

233 3.4. Radiocesium transfer to pine and oak

234 Radiocesium transfer from the outside to the inside of the tree may occur via three routes: the
235 roots, foliage, and bark surface (Ertel and Ziegler, 1991; Tagami et al., 2012). The
236 contribution of bark absorption seems to be low in the pines of the present study because
237 there was no correlation between the radiocesium concentration of the outer bark and the
238 inner parts along the stem. On the other hand, the bark absorption might have occurred in the
239 oaks as there was a significant correlation between the radiocesium concentration in the outer
240 bark and that in the inner parts of these trees.

241 Absorption from the foliar surface, in the case of the Fukushima disaster, might have
242 occurred in evergreens (the pines), but not in deciduous species (the oaks). This is because
243 the disaster occurred during the leafless period for deciduous species. Tagami et al. (2012)
244 reported that woody plants with old leaves at the time of the accident showed higher ^{137}Cs
245 concentrations in newly emerged leaves than did plants without old leaves; however, plants
246 with waxy leaf surfaces had lower concentrations than plants with old leaves without a waxy
247 surface. This suggests that, because pines have waxy leaf surfaces, the contribution of foliar
248 absorption to radiocesium concentration in the pines of the present study was low. The
249 vertically uniform distribution of radiocesium concentration in the inner bark and sapwood of

250 the pines also implies that contamination from the upper part of the tree via foliar absorption
251 was not significant. However, Thiry et al. (2002) estimated that a significant portion of
252 radiocesium incorporation in stem wood was likely due to foliar absorption in the old Scots
253 pines affected by the Chernobyl accident. Furthermore, Tagami and Uchida (2010) reported
254 that trees do not take up large amounts of stable Cs from the soil. Therefore, it is difficult to
255 determine the contribution of foliar absorption to radiocesium concentration in the stems of
256 pines from our results alone.

257 To understand the respective contributions of root, foliar, and bark absorption, periodic
258 monitoring of T_{ag} (aggregated transfer factor) is necessary. The T_{ag} of inner bark and wood
259 (Table 2) were on the same order (10^{-4}) as those reported for the Chernobyl accident (Calmon
260 et al., 2009). However, the present study was conducted during the early stages of
261 radiocesium dynamics and T_{ag} values are changeable. If the T_{ag} values increase with time, the
262 contribution of root absorption can be estimated. On the other hand, if the T_{ag} values do not
263 change significantly, it can be concluded that the dominant route of radiocesium
264 contamination in these trees was foliar or bark absorption.

265

266 4. Conclusion

267 In the early stages of contamination, there was a common pattern in the radial distribution of
268 radiocesium in whole wood in Japanese red pines and Japanese *konara* oaks at different
269 heights. The radiocesium concentration ratio of sapwood to inner bark was significantly
270 different between the species, indicating differential radiocesium allocation and radial
271 transport via rays between the species. The outer bark of oaks had significantly higher
272 radiocesium concentration in the upper stem than in the lower stem, which is likely due to
273 their leafless canopy at the time of the disaster. The radiocesium concentration in the
274 sapwood was vertically constant in the pines, but it was higher in the upper stem than in the

275 lower stem in the oaks. Although the reason is unclear, the vertical contamination pattern in
276 the wood differs between these two species. Further periodic investigations are necessary to
277 reveal the species-specific patterns and mechanisms of radiocesium accumulation in tree
278 stems.

279

280 Acknowledgments

281 We are grateful to the Kawauchi Village office for their permission to conduct this research
282 and their support for our work. The field investigations were greatly assisted by Mr. Y.
283 Kubota and Dr. Y. Maru. The gamma-ray measurement was performed at the Radioisotope
284 Research Center of Kyoto University with helpful advice from Dr. Y. Isozumi and Dr. M.
285 Tosaki. This research was supported by the Environment Research and Technology
286 Development Fund (5ZB-1202) of the Ministry of the Environment, Japan.

287

288

289 References

- 290 Brown, G.N., 1964. Cesium in Liriodendron and other woody species: Organic bonding sites.
291 Science 143, 368–369.
- 292 Calmon, P., Thiry, Y., Zibold, G., Rantavaara, A., Fesenko, S., 2009. Transfer parameter
293 values in temperate forest ecosystems: a review. J. Environ. Radioact. 100, 757–766.
- 294 Cooper, J.A., 1970. Factors determining the ultimate detection sensitivity of Ge(Li)
295 gamma-ray spectrometers. Nucl. Instrum. Methods 82, 273–277.
- 296 Ertel, J., Ziegler, H., 1991. Cs-134/137 contamination and root uptake of different forest trees
297 before and after the Chernobyl accident. Radiat. Environ. Bioph. 30, 147–157.
- 298 Kohno, M., Koizumi, Y., Okumura, K., Mito, I., 1988. Distribution of environmental
299 Cesium-137 in tree rings. J. Environ. Radioact. 8, 15–19.
- 300 Kudo, A., Suzuki, T., Santry, D.C., Mahara, Y., Miyahara, S., Garrec, J.P., 1993. Effectiveness
301 of tree rings for recording Pu history at Nagasaki, Japan. J. Environ. Radioact. 21,
302 55–63.
- 303 Kuroda, K., Kagawa, A., Tonosaki, M., 2013. Radiocesium concentrations in the bark,
304 sapwood and heartwood of three tree species collected at Fukushima forests half a year
305 after the Fukushima Dai-ichi nuclear accident. J. Environ. Radioact. 122, 37–42.
- 306 Ministry of Education, Culture, Sports, Science and Technology (MEXT), 2012. MEXT,
307 Japan. http://radioactivity.nsr.go.jp/ja/contents/7000/6289/24/203_0928.pdf (accessed on
308 July 6, 2013).
- 309 Momoshima, N., Bondietti E.A., 1994. The radial distribution of ⁹⁰Sr and ¹³⁷Cs in trees. J.
310 Environ. Radioact. 22, 93–109.
- 311 Okada, N., Hirakawa, Y., Katayama, Y., 2012. Radial movement of sapwood-injected
312 rubidium into heartwood of Japanese cedar (*Cryptomeria japonica*) in the growing
313 period. J. Wood Sci. 58, 1–8.

314 Soukhova, N.V., Fesenko, S.V., Klein, D., Spiridonov, S.I., Sanzharova, N.I., Badot, P.M.,
315 2003. ^{137}Cs distribution among annual rings of different tree species contaminated after
316 the Chernobyl accident. *J. Environ. Radioact.* 65, 19–28.

317 Tagami, K., Uchida, S., 2010. Can elemental composition data of crop leaves be used to
318 estimate radionuclide transfer to tree leaves? *Radiat. Environ. Biophys.* 49, 583–590.

319 Tagami, K., Uchida, S., Ishii, N., Kagiya, S., 2012. Translocation of radiocesium from stems
320 and leaves of plants and the effect on radiocesium concentrations in newly emerged
321 plant tissues. *J. Environ. Radioact.* 111, 65–69.

322 Thiry, Y., Goor, F., Riesen, T., 2002. The true distribution and accumulation of radiocaesium
323 in stem of Scots pine (*Pinus sylvestris* L.). *J. Environ. Radioact.* 58, 243–259.

324 van Bel, A. J. E., 1990. Xylem-phloem exchange via the rays: the undervalued route of
325 transport. *J. Exp. Bot.* 41, 631–644.

326 Veronica, T., Isozumi, Y., Aoki, T., 1992. Determination of photopeak efficiencies of
327 voluminal samples for the measurement of environmental radioactivities. *Bull. Inst.*
328 *Chem. Res. Kyoto Univ.* 70, 399–407.

329 Yoshida, S., Muramatsu, Y., Dvornik, A. M., Zhuchenko, T. A., Linkov, I., 2004. Equilibrium
330 of radiocesium with stable cesium within the biological cycle of contaminated forest
331 ecosystems. *J. Environ. Radioact.* 75, 301–313.

332 Yoshida, S., Watanabe, M., Suzuki, A., 2011. Distribution of radiocesium and stable elements
333 within a pine tree. *Radiat. Prot. Dosim.* 146, 326–329.

Figure 1

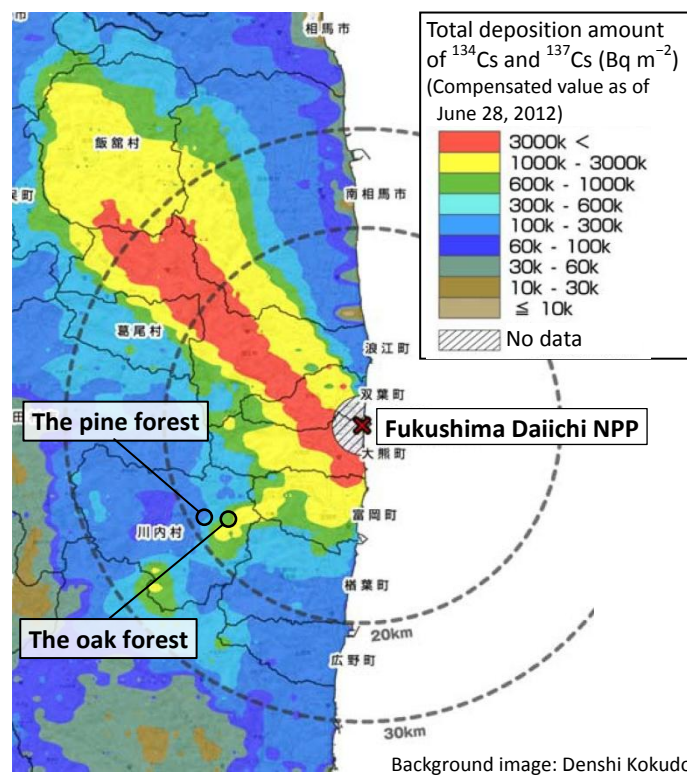


Figure 1. Radiocesium deposition on the ground surface (MEXT, 2012) and locations of study sites. The map has been modified from the original version.

Figure 2

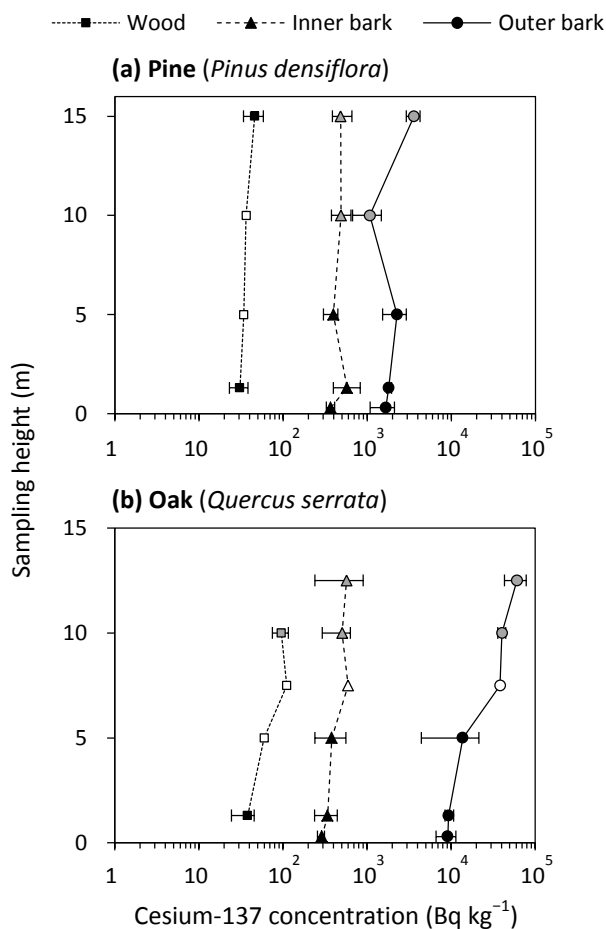


Figure 2. Vertical distribution of ^{137}Cs concentration in each stem part of pines (*Pinus densiflora*) and oaks (*Quercus serrata*). Black symbols are the mean value from three individuals, gray symbols are the mean values from two individuals, and error bars indicate the maximum and minimum values. White symbols show the values from one individual.

Figure 3

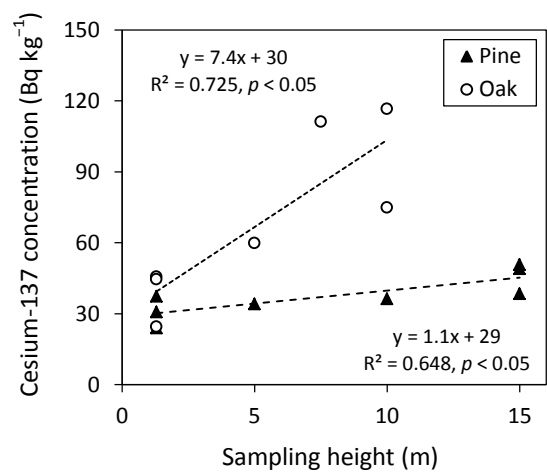


Figure 3. Relationships between the sampling height of wood disk and ¹³⁷Cs concentration in the wood of pines (*Pinus densiflora*) and oaks (*Quercus serrata*).

Figure 4

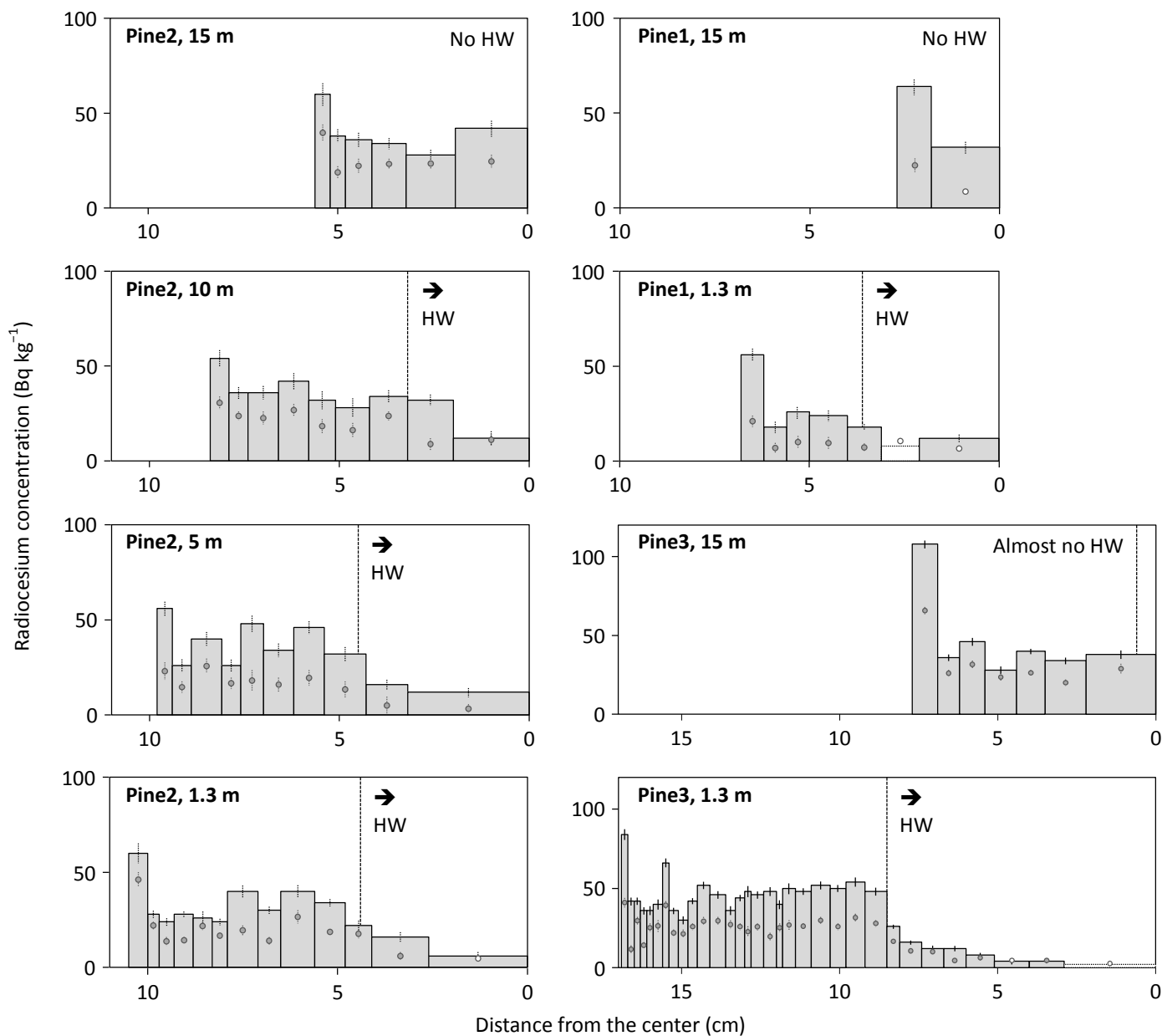


Figure 4. Radial distribution of ^{137}Cs and ^{134}Cs concentrations in wood disks collected at different vertical positions from three pines (*Pinus densiflora*). Gray bars indicate ^{137}Cs concentration and gray circles indicate ^{134}Cs concentration. Error bars indicate standard deviations from counting statistics (σ). White bars and white circles indicate that ^{137}Cs and ^{134}Cs were not detected and show the detection limit. Broken lines indicate the position of the sapwood–heartwood boundary. HW: heart wood.

Figure 5

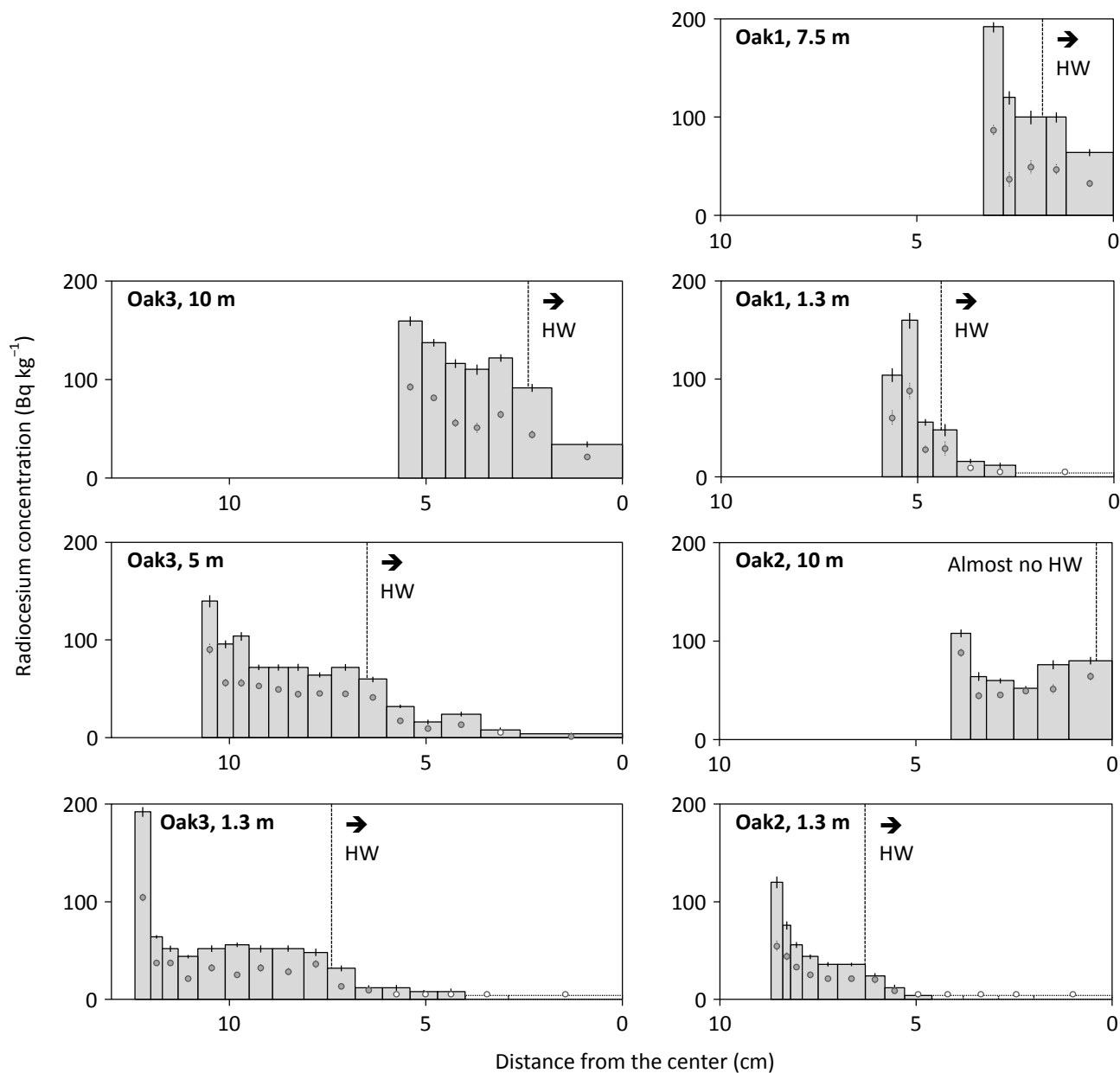


Figure 5. Radial distribution of ¹³⁷Cs and ¹³⁴Cs concentrations in wood disks collected at different vertical positions from three oaks (*Quercus serrata*). Gray bars indicate ¹³⁷Cs concentration and gray circles indicate ¹³⁴Cs concentration. Error bars indicate standard deviations from counting statistics (σ). White bars and white circles indicate that ¹³⁷Cs and ¹³⁴Cs were not detected and show detection limits. Broken lines indicate the position of the sapwood–heartwood boundary. HW: heartwood.

Table 1

Table 1. Description of sample trees.

Species	No.	DBH (cm)	Height (m)	Age (y)
Pine (<i>Pinus densiflora</i>)	1	15.1	17.9	36
	2	25.3	21.7	44
	3	36.9	20.9	54
Oak (<i>Quercus serrata</i>)	1	13.9	11.8	43
	2	20.3	16.7	43
	3	29.2	17.6	43

DBH: diameter at breast height

Table 2

Table 2. Cesium-137 concentration and radioactivity distribution in stem disks collected at 1.3 m above the ground and aggregated transfer factor (T_{ag}) from soil to each stem part

Species	No.	Part ^a	Concentration ^b (Bq kg ⁻¹)	Radioactivity distribution (% of whole disk)	T_{ag} ^c (m ² kg ⁻¹)
Pine (<i>Pinus densiflora</i>)	1	Outer bark	2.0×10^3 (1%)	78	1.7×10^{-2}
		Inner bark	5.0×10^2 (4%)	7	4.2×10^{-3}
		Sapwood	2.9×10 (5%)	14	2.4×10^{-4}
		Heartwood	5.5 (19%)	1	4.7×10^{-5}
	2	Outer bark	1.8×10^3 (1%)	76	1.5×10^{-2}
		Inner bark	4.0×10^2 (5%)	4	3.4×10^{-3}
		Sapwood	3.4×10 (3%)	19	2.9×10^{-4}
		Heartwood	1.2×10 (14%)	1	1.0×10^{-4}
	3	Outer bark	1.7×10^3 (1%)	73	1.4×10^{-2}
		Inner bark	8.3×10^2 (2%)	6	7.0×10^{-3}
		Sapwood	4.6×10 (1%)	19	3.9×10^{-4}
		Heartwood	1.1×10 (5%)	1	8.9×10^{-5}
	Mean	Outer bark	1.8×10^3 (1%)	74	1.5×10^{-2}
Inner bark		5.8×10^2 (2%)	6	4.9×10^{-3}	
Sapwood		3.6×10 (1%)	19	3.1×10^{-4}	
Heartwood		9.4 (5%)	1	7.9×10^{-5}	
Oak (<i>Quercus serrata</i>)	1	Outer bark	1.1×10^4 (1%)	90	5.6×10^{-2}
		Inner bark	4.5×10^2 (2%)	4	2.3×10^{-3}
		Sapwood	9.9×10 (4%)	4	5.2×10^{-4}
		Heartwood	1.8×10 (10%)	2	9.5×10^{-5}
	2	Outer bark	9.0×10^3 (< 1%)	93	4.7×10^{-2}
		Inner bark	3.4×10^2 (3%)	3	1.8×10^{-3}
		Sapwood	5.0×10 (2%)	3	2.7×10^{-4}
		Heartwood	5.7 (12%)	1	3.0×10^{-5}
	3	Outer bark	8.5×10^3 (< 1%)	88	4.4×10^{-2}
		Inner bark	2.4×10^2 (3%)	3	1.3×10^{-3}
		Sapwood	6.6×10 (2%)	8	3.5×10^{-4}
		Heartwood	1.1×10 (9%)	1	5.7×10^{-5}
	Mean	Outer bark	9.4×10^3 (< 1%)	90	4.9×10^{-2}
Inner bark		3.4×10^2 (2%)	3	1.8×10^{-3}	
Sapwood		7.2×10 (1%)	6	3.8×10^{-4}	
Heartwood		1.2×10 (6%)	1	6.1×10^{-5}	

^a Transition part from sapwood to heartwood was included in sapwood.

^b Percentage figures in parentheses are relative standard deviations from counting statistics.

^c Although ¹³⁷Cs in outer bark is not transferred from the soil, T_{ag} was calculated as a reference of deposition.